

Direct Decomposition of NO over Ba–Y_2O_3 Catalyst Prepared by Coprecipitation

Masaaki Haneda,* Yasuyuki Doi, and Masakuni Ozawa

Ceramics Research Laboratory, Nagoya Institute of Technology, 10-6-29 Asahigaoka, Tajimi, Gifu 507-0071

Received August 25, 2011; E-mail: haneda.masaaki@nitech.ac.jp

The catalytic performance of Ba–Y_2O_3 prepared by a coprecipitation method for the direct decomposition of NO was investigated. Although Y_2O_3 catalyzed NO decomposition, its activity was increased by addition of Ba. The maximum NO decomposition activity was achieved on Ba–Y_2O_3 with 5 wt % Ba loading. XRD measurements revealed the formation of a solid solution of Ba and Y_2O_3 as well as $BaCO_3$ small particles, when Ba loading was increased up to 5 wt %. From the comparison between the amount of CO_2 desorption measured by temperature-programmed desorption of CO_2 (CO_2-TPD) and the NO decomposition activity of Ba–Y_2O_3, highly dispersed Ba species, which is initially present as $BaCO_3$ small particles, on the catalyst surface act as catalytically active sites for NO decomposition. On the basis of in situ observation of surface species formed during NO decomposition by Fourier transform infrared (FT-IR) spectroscopy, we proposed that highly dispersed Ba species plays a role for the formation and adsorption of nitrite (NO_2^-) as reactive species for NO decomposition over Ba–Y_2O_3 catalyst.

Catalysis plays a very important role in reducing air pollution caused by nitrogen oxides (NO_x). Of all the catalytic methods to remove NO_x from exhaust gases, direct decomposition of NO ($2NO \rightarrow N_2 + O_2$), which is a thermodynamically favorable reaction, is the most desirable but also the most challenging NO_x abatement process. Numerous studies have been done on this reaction, resulting in the discovery of a wide variety of catalysts, ranging from noble metals to ion-exchanged zeolites.[1,2] Although Cu-ZSM-5 catalyst, which was discovered by Iwamoto et al.,[3] is one of the most effective catalysts, metal oxide based catalysts would be promising candidates for practical application because of their high stability under hydrothermal conditions. However, none has a level of activity that would enable practical application.

Since the early work carried out by Winter,[4] who measured NO decomposition rates on 40 metal oxides, various kinds of metal oxides have been discovered to show activity in this reaction. Boreskov measured the catalytic activity of the fourth period transition-metal oxides for various catalytic reactions such as NO decomposition and CH_4 oxidation, and revealed a close correlation between the activity with respect to NO decomposition and that for homonuclear exchange of oxygen isotopes.[5] This suggests that the activity of the metal oxides for the two reactions is closely related to the lattice metal–oxygen bond strength of the oxides.

On the basis of this knowledge, many metal oxides of which the metal–oxygen bond is weak, such as cobalt oxide,[6–9] oxygen-deficient Sr–Fe oxides,[10] and certain perovskite-type compounds,[11–15] have been extensively investigated. On the other hand, Vannice et al. examined several alkaline earth oxides, which do not include oxygen-deficient sites in the lattice, and found that Sr/La_2O_3 is catalytically active for NO decomposition.[16] Xie et al. also reported that Ba/MgO effectively catalyzes the NO decomposition reaction.[17,18] Recently, Ishihara et al. have investigated the NO decomposition reaction over Ba-containing metal oxide catalysts such as BaMnO-based perovskite oxides,[19,20] Ba/BaY_2O_4,[21] and Ba/Y_2O_3[22] and reported that highly dispersed BaO seems to be active for the direct decomposition of NO. The additive effect of Ba into CeO_2-based mixed oxides was also reported by Iwamoto et al.[23–25] Ba species seems to be a promising catalytically active species for the direct decomposition of NO.

One of the authors has investigated the catalytic performance of supported alkaline earth metal oxides for NO decomposition and found that Y_2O_3 is the most effective support and Ba/Y_2O_3 shows the highest NO decomposition activity, which decreased in the order of Ba/Y_2O_3 > Sr/Y_2O_3 > Ca/Y_2O_3 > Mg/Y_2O_3 > Y_2O_3.[26] We also proposed the importance of the basicity of Ba/Y_2O_3 for NO decomposition to occur. However, the state of Ba species and its essential role as a catalytically active site has not been clarified so far. In the present work, we have investigated the catalytic performance of Ba-doped Y_2O_3 having well-controlled structure prepared by a coprecipitaion method for NO decomposition. A catalytically active site of Ba–Y_2O_3 is discussed on the basis of the reaction data as well as catalyst characterizations.

Experimental

Ba-Doped Y_2O_3 was prepared by coprecipitation using $(NH_4)_2CO_3$ as a precipitation agent, with an aqueous solution of yttrium(III) nitrate and barium(II) nitrate. The precipitate thus obtained was washed with distilled water, followed by drying at 383 K and calcination at 873 K for 5 h in air. The loading of Ba was changed from 1 to 15 wt %. The samples are expressed as Ba(x)–Y_2O_3, where x is the loading of Ba.

Published on the web December 6, 2011; doi:10.1246/bcsj.20110258

The direct decomposition of NO was carried out in a fixed-bed continuous flow reactor. The reaction gas composed of 1000 ppm NO with He as the balance gas was fed to a 0.5 g catalyst at a rate of 30 $cm^3 min^{-1}$ ($W/F = 1.0\,g\,s\,cm^{-3}$). The effluent gas was analyzed by gas chromatography (Shimadzu GC-8A) using a Molecular Sieve 5A column (for analysis of O_2 and N_2) and a Porapak Q column (for analysis of N_2O). A chemiluminescence NO_x analyzer (Shimadzu NOA-305A) was used to check the stability of the catalytic activity. The catalytic activity was measured after the reaction was started in 2 h at each temperature.

The BET surface area of the samples was determined using a conventional flow apparatus (Micromeritics ASAP2010) by nitrogen adsorption at liquid nitrogen temperature. The crystal structure of the samples was identified by XRD (Rigaku MiniFlexII) measurements using Cu Kα radiation at 30 kV and 15 mA.

Temperature-programmed desorption of CO_2 (CO_2-TPD) was performed using an atmospheric flow system (BELCAT, BEL Japan). Before each CO_2-TPD measurement, the sample was pretreated in a flow of He at 873 K for 1 h and then cooled down to 323 K. CO_2 adsorption was performed by passing a gas mixture of 0.5% CO_2/He through the sample bed at 323 K for 1 h. After the adsorption gas was purged with He to remove physically adsorbed CO_2, TPD measurement was carried out up to 873 K at a heating rate of 10 K min^{-1} in flowing He at a flow rate of 30 $cm^3 min^{-1}$. A quadrupole mass spectrometer (M-201QA-TDM, Canon Anelva) was used to analyze the desorbed CO_2.

The diffuse reflectance FT-IR spectra were recorded using a Nicolet 6700 FT-IR spectrometer, accumulating 64 scans at a resolution of 4 cm^{-1}. Prior to each experiment, 25 mg of a catalyst placed in a diffuse reflectance high temperature cell (Spectra Tech) fitted with CaF_2 windows was pretreated in situ by heating in flowing He at 873 K, followed by changing to the desired temperature. The background spectrum of the clean surface was measured for spectra correction. The reaction gas containing either 1000 ppm NO or 0.5% CO_2 diluted with He was fed to the catalyst at a flow rate of 30 $cm^3 min^{-1}$.

Results and Discussion

NO Decomposition Activity of Ba–Y_2O_3. Figure 1 shows the temperature dependence of N_2, O_2, and N_2O yield for NO decomposition over Ba(5)–Y_2O_3 catalyst, where the activity was measured by increasing the reaction temperature from 873 to 1173 K in steps of 50 K. The formation of N_2 was observed at the reaction temperatures above 923 K and then monotonously increased with increasing reaction temperature. N_2O as a product for NO decomposition was hardly formed in the entire temperature range. O_2 was always formed at a steady-state with an O_2/N_2 ratio of approximately unity, suggesting that NO decomposition proceeds catalytically.

Figure 2 shows the catalytic activity of Ba–Y_2O_3 with different Ba loadings for NO decomposition. The O_2/N_2 ratio was found to be approximately unity irrespective of catalyst samples. As can be seen in Figure 2, Y_2O_3 itself was found to catalyze NO decomposition. Its activity increased with increasing reaction temperature. However, it is noteworthy that NO decomposition over Y_2O_3 was significantly promoted by addition of Ba. The activity of Ba–Y_2O_3 increased with increasing Ba loading, and reached a maximum at the Ba loading of 5 wt %.

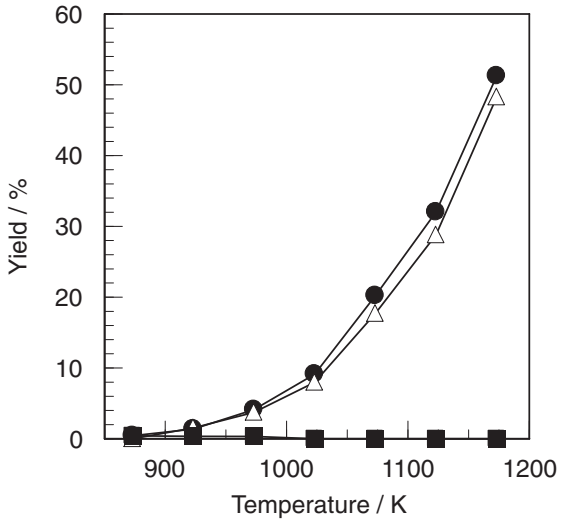

Figure 1. Temperature dependence of N_2, O_2, and N_2O yield for NO decomposition over Ba(5)–Y_2O_3 catalyst. Conditions: NO = 1000 ppm, gas flow rate = 30 $cm^3 min^{-1}$, and $W/F = 1.0\,g\,s\,cm^{-3}$. (●) N_2 yield, (△) O_2 yield, and (■) N_2O yield.

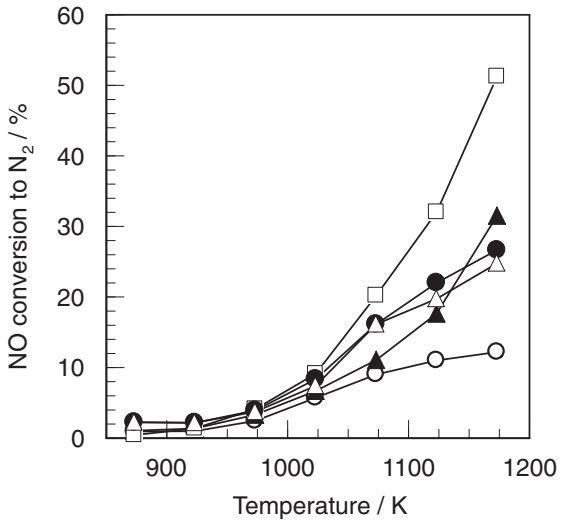

Figure 2. Activity of Ba–Y_2O_3 with various Ba loadings for NO decomposition. (○) Y_2O_3, (▲) Ba(1)–Y_2O_3, (□) Ba(5)–Y_2O_3, (●) Ba(10)–Y_2O_3, and (△) Ba(15)–Y_2O_3. The reaction conditions are the same as those for Figure 1.

Physicochemical Properties of Ba–Y_2O_3. Figure 3 shows the XRD patterns of Ba–Y_2O_3 with different Ba loadings. Y_2O_3 showed distinct XRD peaks indexed to the cubic phase. No phase other than Y_2O_3 has been formed (Figure 3a). As can be seen in Figure 3b, the addition of 1 wt % Ba into Y_2O_3 caused a shift of XRD peaks due to Y_2O_3 toward lower angles, suggesting the formation of a solid solution in which Ba^{2+} ions are incorporated into Y_2O_3 lattice. This peak shift can be explained by the fact that the radius of Ba^{2+} ion (0.135 nm) is larger than that of Y^{3+} ion (0.09 nm). It is of interest that no

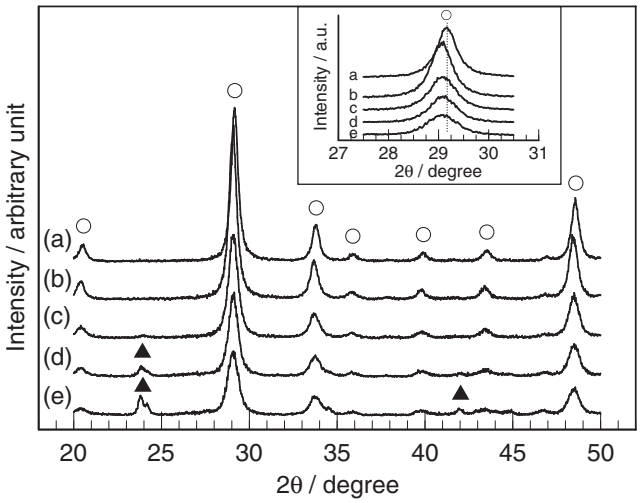

Figure 3. XRD patterns of Ba–Y_2O_3 with various Ba loadings. (a) Y_2O_3, (b) Ba(1)–Y_2O_3, (c) Ba(5)–Y_2O_3, (d) Ba(10)–Y_2O_3, and (e) Ba(15)–Y_2O_3. (○) for Y_2O_3 and (▲) for $BaCO_3$.

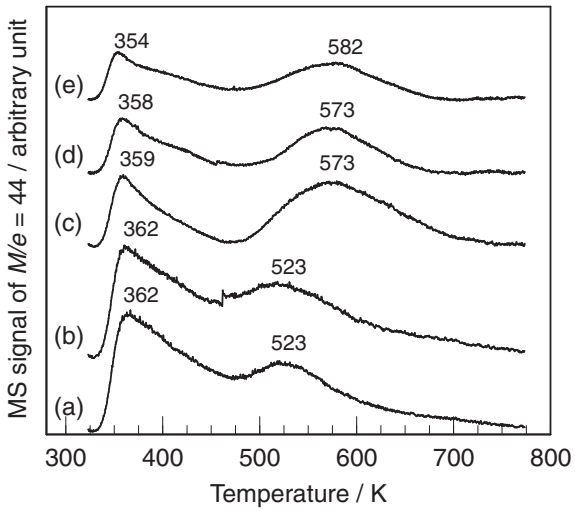

Figure 4. CO_2-TPD profiles of Ba–Y_2O_3 with various Ba loadings. (a) Y_2O_3, (b) Ba(1)–Y_2O_3, (c) Ba(5)–Y_2O_3, (d) Ba(10)–Y_2O_3, and (e) Ba(15)–Y_2O_3.

Table 1. BET Surface Area of Ba–Y_2O_3 Samples

Catalyst	BET surface area/$m^2\,g^{-1}$
Y_2O_3	34.8
Ba(1)–Y_2O_3	39.9
Ba(5)–Y_2O_3	27.1
Ba(10)–Y_2O_3	20.9
Ba(15)–Y_2O_3	20.1

further shift of XRD peaks due to Y_2O_3 was observed for the Ba–Y_2O_3 samples with Ba loading more than 5 wt % (Figure 3c). This suggests that a small amount of Ba^{2+} ions can substitute with Y^{3+} ions in Y_2O_3 lattice. As seen in Figure 3c, new peaks assignable to $BaCO_3$ were detected when Ba loading was increased up to 5 wt %. Ba^{2+} ions which were not substituted with Y^{3+} ions seem to be present as $BaCO_3$. The intensity of XRD peaks due to $BaCO_3$ increased with increasing Ba loading, suggesting an agglomeration of $BaCO_3$ particles.

Table 1 summarizes the BET surface area of Ba–Y_2O_3 samples. Interestingly, the BET surface was increased by addition of a small amount of Ba (1 wt %). As described above, an inhibition of Y_2O_3 sintering is probably due to the formation of a solid solution of Ba and Y_2O_3. The addition of more than 5 wt % Ba caused a decrease of BET surface area. Since Ba(5)–Y_2O_3 showed the highest NO decomposition activity, the BET surface area does not seem to be responsible for high NO decomposition activity.

One of the authors has reported that the catalytic activity of alkaline earth metal-doped Co_3O_4 catalysts for NO decomposition is directly related to not only the amount of surface basic sites, which corresponds to the surface density of alkaline earth metal species, but also the strength of basicity.[27] Taking into account the results of XRD measurements (Figure 3), the dispersion state of Ba species in the Ba–Y_2O_3 samples seems to be different depending on Ba loading. In order to gain information on the amount of Ba species exposed on Y_2O_3 surface, CO_2-TPD measurements were carried out. Figure 4 shows the CO_2-TPD profiles of Ba–Y_2O_3 samples with different Ba loadings. Y_2O_3 gave two CO_2 desorption peaks at 362 and 523 K, indicating the presence of surface basic sites. No significant change in CO_2-TPD profile was observed for Ba(1)–Y_2O_3 (Figure 4b), suggesting that 1 wt % Ba additive does not affect the basicity of Y_2O_3. This is probably because most of Ba species are incorporated into Y_2O_3 lattice to form a solid solution.

When Ba loading was increased up to 5 wt %, an appearance of a new CO_2 desorption peak was observed at 573 K (Figure 4c), indicating the presence of strong basic sites. This peak is probably due to the desorption of CO_2 adsorbed on Ba species dispersed on Y_2O_3 surface. When Ba loading was increased up to more than 10 wt %, a decrease in the CO_2 desorption peak ascribed to an agglomeration of Ba species was observed. Figure 5 shows the change in the amount of desorbed CO_2 at around 523–623 K, as well as the rate of N_2 formation at 1073 K, as a function of Ba loading. Relatively good correlation between the amount of desorbed CO_2 and the NO decomposition activity was observed, suggesting that the amount of Ba species exposed on the catalyst surface is one of the important factors to determine the NO decomposition activity of Ba–Y_2O_3 catalyst.

Stability of Ba(5)–Y_2O_3 Catalyst. In order to obtain information on the stability of Ba(5)–Y_2O_3, the activity was continuously measured from 1173 to 873 K in steps of 50 K after measuring the activity under the condition of increasing reaction temperature. Figure 6 compares the activity of Y_2O_3 and Ba(5)–Y_2O_3 measured under the conditions of increasing and decreasing reaction temperature. The NO decomposition activity of Y_2O_3 under the latter condition was lower than that under the former condition. This is probably due to a loss of active sites by sintering of Y_2O_3 during the reaction at 1173 K. On the other hand, interestingly, the activity of Ba(5)–Y_2O_3 was significantly increased when the reaction temperature was decreased from 1173 to 873 K. This clearly suggests that the catalytically active sites in Ba(5)–Y_2O_3 were created during the reaction at 1173 K.

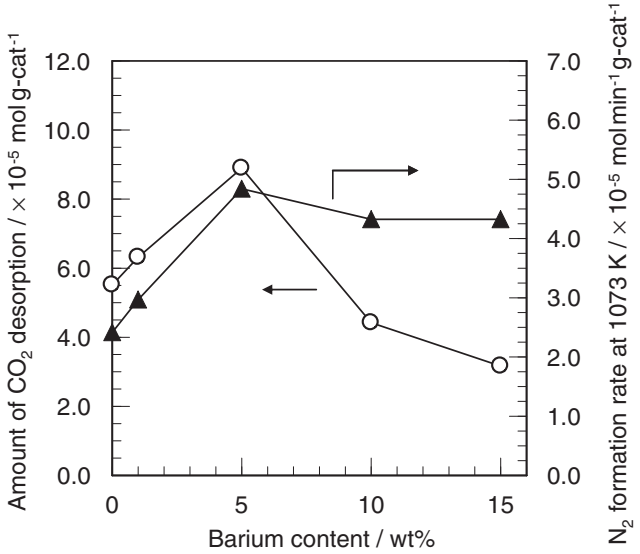

Figure 5. Change in the amount of CO_2 desorption (○) and the rate of N_2 formation at 1073 K (▲) over Ba–Y_2O_3 as a function of barium content.

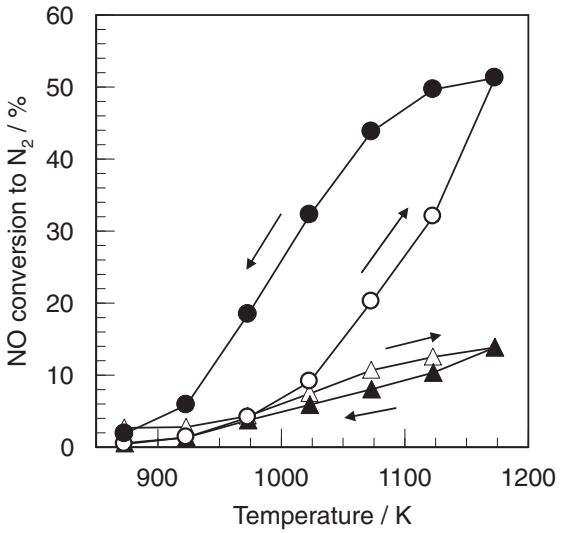

Figure 6. Comparison of the activity for NO decomposition measured under the condition of increasing (△, ○) and decreasing (▲, ●) reaction temperature over Y_2O_3 (△, ▲) and Ba(5)–Y_2O_3 (○, ●). The reaction conditions are the same as those for Figure 1.

The time dependence of NO conversion on Ba(5)–Y_2O_3 was measured at 1173 K in order to understand the creation of catalytically active sites. Figure 7 shows the change in the NO conversion to N_2, as well as the amount of CO_2 evolved, as a function of time on stream. Obviously, the NO conversion to N_2 continuously increased with increasing the reaction time. More than 30 h were needed to reach stable activity. In contrast, a continuous decrease of the amount of CO_2 evolved was observed. Figure 8 shows the XRD patterns of Ba(5)–Y_2O_3 samples before and after the reaction. It appears that the XRD peaks assignable to $BaCO_3$ completely disappeared after the reaction. On the other hand, an appearance of weak XRD peaks ascribed to BaY_2O_4 was observed, suggesting that the decomposition of $BaCO_3$ and subsequent reaction with Y_2O_3 to form BaY_2O_4 proceed during the decomposition reaction.

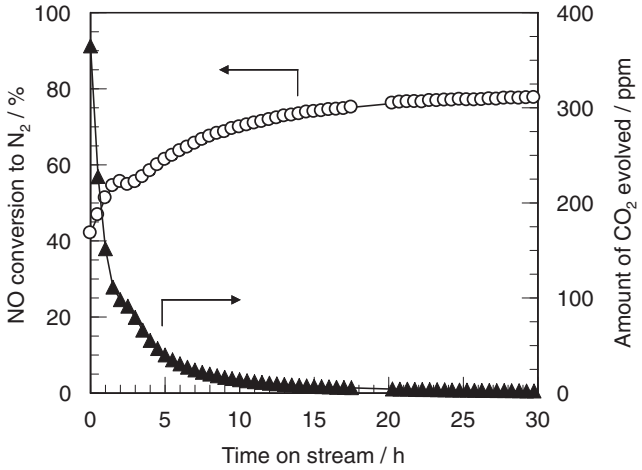

Figure 7. Time dependence of the conversion of NO to N_2 (○) and the amount of CO_2 evolved (▲) at 1173 K over Ba(5)–Y_2O_3. The reaction conditions are the same as those for Figure 1.

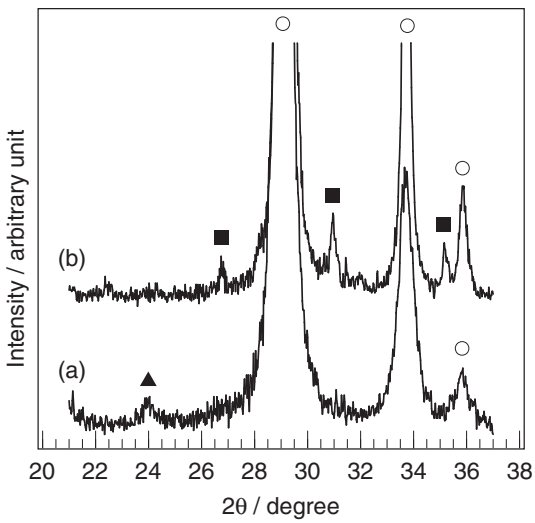

Figure 8. XRD patterns of Ba(5)–Y_2O_3: (a) fresh, (b) after use in the reaction. (○) for Y_2O_3, (▲) for $BaCO_3$, and (■) for BaY_2O_4.

Goto et al. reported that BaY_2O_4 itself with very low surface area ($<1\,m^2\,g^{-1}$) is not an effective catalyst for NO decomposition.[21] On the other hand, in the present study, the crystallite size of BaY_2O_4 was estimated to be ca. 20 nm from an XRD peak at $2\theta = 30.9°$ using Scherrer's equation, indicating the presence of BaY_2O_4 small particles dispersed on Y_2O_3 surface. Taking into account the fact that the activity of Ba(5)–Y_2O_3 continuously increased with the reaction time (Figure 7), highly dispersed Ba species in the form of BaY_2O_4 small particles is considered to play an important role as the catalytically active sites for NO decomposition.

State of Ba Species in Ba(5)–Y_2O_3 as Catalytically Active Sites. CO_2 is known to be specifically adsorbed on basic sites of metal oxides, giving rise to a variety of carbonate-like species depending on the geometric configuration of adsorption

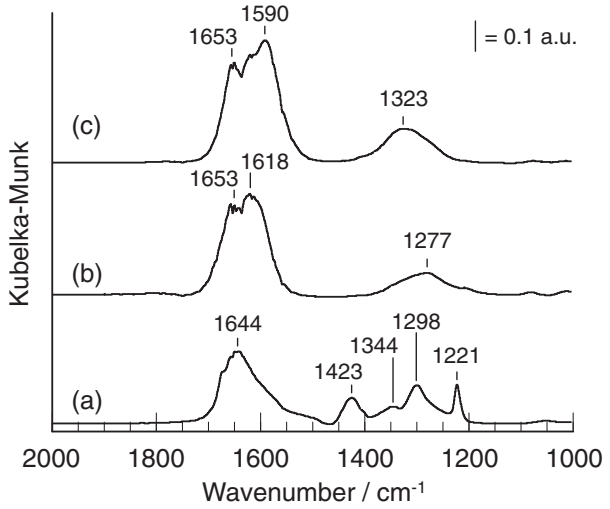

Figure 9. Diffuse reflectance FT-IR spectra of CO_2 species adsorbed on (a) Y_2O_3, (b) Ba(5)–Y_2O_3, and (c) Ba(5)–Y_2O_3 pretreated in He at 1173 K for 8 h. All the samples were treated with He at 873 K for 2 h, followed by exposure to 0.5% CO_2/He at room temperature for 25 min.

sites.[28] The surface state of Ba species in Ba–Y_2O_3 was then examined by CO_2 adsorption followed by FT-IR spectroscopy. Figure 9 shows FT-IR spectra of CO_2 species adsorbed on Y_2O_3 and Ba(5)–Y_2O_3. The exposure of CO_2 to Y_2O_3 caused an appearance of IR bands at 1644, 1423, 1344, 1298, and 1221 cm^{-1} (Figure 9a). The IR bands at 1644 and 1298 cm^{-1} with a shoulder at 1344 cm^{-1} are characteristic for bidentate carbonates coordinated with coordinatively unsaturated (*cus*) Y^{3+}–O^{2-} pair sites.[29] The bands at 1423 and 1221 cm^{-1} can be assigned to monodentate carbonates[30] and hydrogen carbonates formed by adsorption on surface OH groups of Y_2O_3,[28] respectively. When CO_2 was adsorbed on Ba(5)–Y_2O_3, a different IR spectrum from that for Y_2O_3 was observed (Figure 9b). This is probably because CO_2 is preferentially adsorbed on more strongly basic sites of Ba species. According to the previous report,[31] a pair of the bands at 1618 and 1277 cm^{-1} can be assigned to bidentate carbonates bridged on Ba sites. A shift of IR band at 1644 cm^{-1} detected for Y_2O_3 to 1653 cm^{-1} was observed. This is probably due to perturbations caused by interaction of Ba and Y_2O_3. Therefore, a shoulder band at 1653 cm^{-1} can be ascribed to bidentate carbonates bridged on *cus* Y^{3+} and Ba sites.

As described above, the catalytically active Ba species, which may be in a highly dispersed state in the form of BaY_2O_4 small particles, are created via the decomposition of $BaCO_3$ by the reaction gas treatment of Ba–Y_2O_3 at 1173 K. In order to gain information on the status of catalytically active Ba species, FT-IR spectra of CO_2 species adsorbed on Ba(5)–Y_2O_3 pretreated with He at 1173 K for 8 h were measured. In another set of experiments, we have recognized that $BaCO_3$ dispersed on Y_2O_3 is completely decomposed by He treatment at 1173 K for 8 h and then NO conversion at 1173 K is as high as 70%. As shown in Figure 9c, similar IR spectrum with that obtained for Ba(5)–Y_2O_3 without pretreatment was obtained. However, a shift of IR bands due to bidentate carbonates bridged on Ba sites was clearly observed. Namely, a pair of the bands at 1618 and 1277 cm^{-1} shifted to 1590 and 1323 cm^{-1}, respectively. It appears that the value of $\Delta\nu$(C–O) splitting between symmetric and asymmetric stretching modes of carbonate species was changed from 341 to 267 cm^{-1} by He treatment at 1173 K.

The $\Delta\nu$(C–O) splitting is known to be in relation with the distortion of the CO_3^{2-} ion. The value of $\Delta\nu$(C–O) splitting for CO_2 species adsorbed on Ba(5)–Y_2O_3 was different depending on the history of the sample, namely with or without He treatment at 1173 K. This suggests that geometric configuration of Ba species on Y_2O_3 surface is altered by He treatment at 1173 K. Busca and Lorenzelli proposed that the adsorbed state of carbonate species with a small $\Delta\nu$(C–O) splitting is more stable than that with a large $\Delta\nu$(C–O) splitting.[32] Daturi et al. reported that the difference in stability of carbonate species having a different $\Delta\nu$(C–O) splitting formed on mixed metal oxides would be governed by the potentiality of the relaxation of surface ions.[33] Namely, a homogeneous mixture of metal oxide ions may be favorable for the relaxation of surface ions, giving carbonate species with more stable adsorbed state. The small $\Delta\nu$(C–O) splitting for Ba(5)–Y_2O_3 with He treatment at 1173 K suggests the formation of highly dispersed Ba species interacting strongly with Y_2O_3. This consideration is in good agreement with our XRD results in which the formation of BaY_2O_4 small particles was observed for Ba(5)–Y_2O_3 after use in the NO decomposition reaction (Figure 8). Taking into account the fact that the activity of Ba(5)–Y_2O_3 for NO decomposition was continuously increased with increasing the reaction time (Figure 7), highly dispersed Ba species interacting strongly with Y_2O_3 is considered to play an important role as the catalytically active sites for NO decomposition.

Observation of NO Species Adsorbed on Ba(5)–Y_2O_3 by FT-IR. One of the authors has extensively studied in situ FT-IR spectroscopy and isotopic transient kinetic analysis for NO decomposition over alkali metal- and alkaline earth metal-doped Co_3O_4 catalysts, and proposed the reaction mechanism that nitrite (NO_2^-) species formed on alkali metal or alkaline earth metal participates as a reaction intermediate in NO decomposition.[34,35] Xie et al. reported that the nitrate (NO_3^-) species formed on Ba/MgO is a spectator species in NO decomposition reaction and poisons the reaction sites to which it is strongly adsorbed.[17,18] They also proposed a reaction mechanism of NO decomposition over Ba/MgO, where the gas-phase NO reacts with a surface NO_x species such as NO_2^- on the barium surface. Therefore, we suspect the formation of NO_2^- species and the participation as a reaction intermediate for NO decomposition over Ba–Y_2O_3 catalyst.

In order to confirm this idea, the surface species formed during NO decomposition over Y_2O_3, Ba(5)–Y_2O_3, and Ba(15)–Y_2O_3 pretreated in He at 1173 K for 8 h were measured using diffuse reflectance FT-IR spectrometer. As shown in Figure 10A(a), distinct IR bands appeared at 1408, 1307, 1212, and 1196 cm^{-1} when 1000 ppm NO/He flowing gas was exposed toY_2O_3 at 673 K. A pair of IR bands at 1408 and 1307 cm^{-1} can be assigned to monodentate NO_2^- species adsorbed on Y_2O_3, while the latter two bands to bridged NO_2^- species.[36] These bands decreased with increasing the reaction temperature and then completely disappeared at 873 K. As can be seen in Figure 10B, a sharp IR band assignable to NO_2^- species adsorbed on Ba sites[37] was detected at 1194 cm^{-1} for

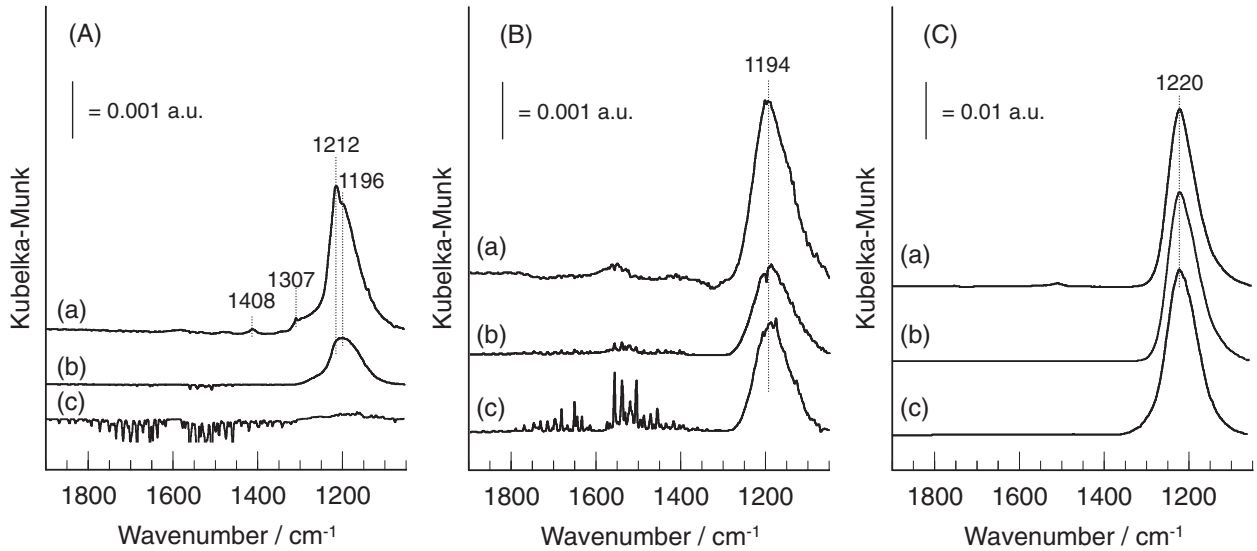

Figure 10. Diffuse reflectance FT-IR spectra recorded in flowing 1000 ppm NO/He over (A) Y_2O_3, (B) Ba(5)–Y_2O_3, and (C) Ba(15)–Y_2O_3, which was treated in He at 1173 K for 8 h at (a) 673, (b) 773, and (c) 873 K for 30 min.

Ba(5)–Y_2O_3. Its band intensity decreased with increasing temperature, but it was still observed at 873 K. Taking into account the fact that IR bands due to NO_2^- species completely disappeared over Y_2O_3 at 873 K (Figure 10A(c)), Ba plays an important role for the formation, adsorption, and stabilization of NO_2^- species. On the other hand, the exposure of NO/He flowing gas to Ba(15)–Y_2O_3 gave rise to the appearance of a different IR band at 1220 cm^{-1} (Figure 10C). According to the previous report,[38,39] the IR band at 1220 cm^{-1} can be assigned to monodentate NO_3^- species adsorbed on Ba sites. No siginificant change in the IR band was observed as the temperature increased to 873 K, suggesting that NO_3^- species is a very stable species. This is in agreement with the reports by Xie et al.[17,18] in which NO_3^- species formed on Ba/MgO was proposed to be a spectator species in NO decomposition. The lower activity of Ba(15)–Y_2O_3 for NO decomposition (Figure 2) would be ascribed to the preferential formation of NO_3^- species.

In conclusion, highly dispersed Ba species, which is preferentially present in Ba(5)–Y_2O_3, interacting strongly with Y_2O_3 plays an important role for the formation, adsorption, and stabilization of NO_2^- species as a reaction intermediate in NO decomposition, leading to high NO decomposition activity.

Conclusion

Although Y_2O_3 shows NO decomposition activity, the addition of Ba causes a significant promotion of NO decomposition reaction. An optimal Ba loading is 5 wt%. Catalytic activity of Ba–Y_2O_3 is related to the number of basic sites, which can be estimated from the amount of CO_2 desorption in CO_2-TPD, suggesting that the presence of highly dispersed Ba species on the catalyst surface is essential for NO decomposition to proceed. In situ FT-IR spectroscopy suggested that Ba plays an important role for the formation and adsorption of NO_2^- species as a reaction intermediate in NO decomposition.

This study was supported by a Grant-in-Aid for Scientific Research (No. 22350068) from the Ministry of Education, Culture, Sports, Science and Technology of Japan.

References

1 M. Iwamoto, H. Hamada, *Catal. Today* **1991**, *10*, 57.
2 F. Garin, *Appl. Catal., A* **2001**, *222*, 183.
3 M. Iwamoto, H. Furukawa, Y. Mine, F. Uemura, S.-i. Mikuriya, S. Kagawa, *J. Chem. Soc., Chem. Commun.* **1986**, 1272.
4 E. R. S. Winter, *J. Catal.* **1971**, *22*, 158.
5 G. K. Boreskov, *Discuss. Faraday Soc.* **1966**, *41*, 263.
6 H. C. Yao, M. Shelef, in *The Catalytic Chemistry of Nitrogen Oxides*, ed. by R. M. Klimisch, J. G. Larson, Plenum Press, London, **1975**, p. 45.
7 A. Amirnazmi, J. E. Benson, M. Boudart, *J. Catal.* **1973**, *30*, 55.
8 H. Hamada, Y. Kintaichi, M. Sasaki, T. Ito, *Chem. Lett.* **1990**, 1069.
9 P. W. Park, J. K. Kil, H. H. Kung, M. C. Kung, *Catal. Today* **1998**, *42*, 51.
10 S. Shin, Y. Hatakeyama, K. Ogawa, K. Shimomura, *Mater. Res. Bull.* **1979**, *14*, 133.
11 H. Shimada, S. Miyama, H. Kuroda, *Chem. Lett.* **1988**, 1797.
12 H. Yasuda, N. Mizuno, M. Misono, *J. Chem. Soc., Chem. Commun.* **1990**, 1094.
13 Y. Teraoka, T. Harada, S. Kagawa, *J. Chem. Soc., Faraday Trans.* **1998**, *94*, 1887.
14 Y. Zhu, D. Wang, F. Yuan, G. Zhang, H. Fu, *Appl. Catal., B* **2008**, *82*, 255.
15 S. Tsujimoto, K. Mima, T. Masui, N. Imanaka, *Chem. Lett.* **2010**, *39*, 456.
16 M. A. Vannice, A. B. Walters, X. Zhang, *J. Catal.* **1996**, *159*, 119.
17 S. Xie, G. Mestl, M. P. Rosynek, J. H. Lunsford, *J. Am. Chem. Soc.* **1997**, *119*, 10186.
18 S. Xie, M. P. Rosynek, J. H. Lunsford, *J. Catal.* **1999**, *188*, 24.

19 H. Iwakuni, Y. Shinmyou, H. Yano, H. Matsumoto, T. Ishihara, *Appl. Catal., B* **2007**, *74*, 299.
20 H. Iwakuni, Y. Shinmyou, H. Yano, K. Goto, H. Matsumoto, T. Ishihara, *Bull. Chem. Soc. Jpn.* **2008**, *81*, 1175.
21 K. Goto, H. Matsumoto, T. Ishihara, *Top. Catal.* **2009**, *52*, 1776.
22 T. Ishihara, K. Goto, *Catal. Today* **2011**, *164*, 484.
23 S. Iwamoto, R. Takahashi, M. Inoue, *Appl. Catal., B* **2007**, *70*, 146.
24 W.-J. Hong, S. Iwamoto, M. Inoue, *Catal. Lett.* **2010**, *135*, 190.
25 W.-J. Hong, S. Iwamoto, S. Hosokawa, K. Wada, H. Kanai, M. Inoue, *J. Catal.* **2011**, *277*, 208.
26 G. Tsuboi, M. Haneda, Y. Nagao, Y. Kintaichi, H. Hamada, *J. Jpn. Pet. Inst.* **2005**, *48*, 53.
27 M. Haneda, G. Tsuboi, Y. Nagao, Y. Kintaichi, H. Hamada, *Catal. Lett.* **2004**, *97*, 145.
28 J. C. Lavalley, *Catal. Today* **1996**, *27*, 377.
29 C. Morterra, G. Cerrato, L. Ferroni, *J. Chem. Soc., Faraday Trans.* **1995**, *91*, 125.
30 T. Viinikainen, H. Rönkkönen, H. Bradshaw, H. Stephenson, S. Airaksinen, M. Reinikainen, P. Simell, O. Krause, *Appl. Catal., A* **2009**, *362*, 169.
31 F. Frola, M. Manzoli, F. Prinetto, G. Ghiotti, L. Castoldi, L. Lietti, *J. Phys. Chem. C* **2008**, *112*, 12869.
32 G. Busca, V. Lorenzelli, *Mater. Chem.* **1982**, *7*, 89.
33 M. Daturi, C. Binet, J.-C. Lavalley, A. Galtayries, R. Sporken, *Phys. Chem. Chem. Phys.* **1999**, *1*, 5717.
34 M. Haneda, Y. Kintaichi, H. Hamada, *Appl. Catal., B* **2005**, *55*, 169.
35 M. Haneda, I. Nakamura, T. Fujitani, H. Hamada, *Catal. Surv. Asia* **2005**, *9*, 207.
36 A. A. Davydov, in *Infrared Spectroscopy of Adsorbed Species on the Surface of Transition Metal Oxides*, ed. by C. H. Rochester, John Wiley & Sons, Chichester, **1990**, pp. 53–56.
37 P. T. Fanson, M. R. Horton, W. N. Delgass, J. Lauterbach, *Appl. Catal., B* **2003**, *46*, 393.
38 N. Maeda, A. Urakawa, A. Baiker, *J. Phys. Chem. C* **2009**, *113*, 16724.
39 I. S. Pieta, M. García-Diéguez, C. Herrera, M. A. Larrubia, L. J. Alemany, *J. Catal.* **2010**, *270*, 256.